



SARS-CoV-2 B.1.1.7 Infection of Syrian Hamster Does Not Cause More Severe Disease, and Naturally Acquired Immunity Confers Protection

Ivette A. Nuñez,^a Christopher Z. Lien,^a Prabhuanand Selvaraj,^a Charles B. Stauff,^a  Shufeng Liu,^a Matthew F. Starost,^b  Tony T. Wang^a

^aDivision of Viral Products, Center for Biologics Evaluation and Research, Food and Drug Administration, Silver Spring, Maryland, USA

^bDivision of Veterinary Resources, Diagnostic and Research Services Branch, National Institutes of Health, Bethesda, Maryland, USA

Ivette A. Nuñez, Christopher Z. Lien, and Prabhuanand Selvaraj contributed equally; author order was determined both alphabetically and in order of increasing seniority.

ABSTRACT Epidemiological studies have revealed the emergence of multiple severe acute respiratory syndrome coronavirus 2 (SARS-CoV-2) variants of concern (VOC), including the lineage B.1.1.7 that is rapidly replacing old variants. The B.1.1.7 variant has been linked to increased morbidity rates, transmissibility, and potentially mortality. To assess viral fitness *in vivo* and to address whether the B.1.1.7 variant is capable of immune escape, we conducted infection and reinfection studies in naive and convalescent Syrian hamsters (>10 months old). Nasal wash samples from hamsters infected by a B.1.1.7 variant exhibited slightly higher viral RNA levels but lower infectious titers than those from B.1 (G614) variant-infected hamsters, and the two variants induced comparable lung pathologies in hamsters. Despite a sporadic and transient low-level infection in the nasal cavity, convalescent hamsters that had recovered from a previous USA-WA1 isolate (D614) infection displayed no observable clinical signs or lung pathology following B.1.1.7 rechallenge. Altogether, our study did not find that the B.1.1.7 variant significantly differs from the B.1 variant in pathogenicity in Syrian hamsters and that a heterologous natural infection-induced immunity confers protection against a secondary challenge by the B.1.1.7 variant.

IMPORTANCE The rapid emergence of several variants of concern of SARS-CoV-2 calls for evaluations of viral fitness and pathogenicity in animal models in order to understand the mechanism of enhanced transmission and the possible increases in morbidity and mortality rates. Here, we demonstrated that immunity naturally acquired through a prior infection with the first-wave variant does confer nearly complete protection against the B.1.1.7 variant in Syrian hamsters upon reexposure. Strikingly, although the B.1.1.7 variant appears to replicate to a higher level in the nose than the ancestral B.1 variant, it does not induce more severe lung pathology in hamsters.

KEYWORDS SARS-CoV-2 variants, B.1.1.7, COVID-19, spike protein, Syrian hamster

Despite the proofreading activity provided by the 3'-to-5' exonuclease activity of nonstructural protein 14, SARS-CoV-2 has accumulated multiple mutations in its viral genome (1). Mutations occurring in the spike protein are of major concern due to the role of this glycoprotein in mediating virus entry and as the major target of neutralizing antibodies (2–5). In March of 2020, the D614G SARS-CoV-2 B.1 variant emerged and became the predominant strain of virus throughout Europe and the United States (6). Since late fall 2020, the emergent B.1.1.7 SARS-CoV-2 variant became predominant in the United Kingdom and contributed to the December surge in positive SARS-CoV-2 cases and the increase in hospitalization and death rates (7). Among the 10 mutations/deletions found in the spike protein of the B.1.1.7 variant, the N501Y mutation has

Citation Nuñez IA, Lien CZ, Selvaraj P, Stauff CB, Liu S, Starost MF, Wang TT. 2021. SARS-CoV-2 B.1.1.7 infection of Syrian hamster does not cause more severe disease, and naturally acquired immunity confers protection. *mSphere* 6:e00507-21. <https://doi.org/10.1128/mSphere.00507-21>.

Editor Michael J. Imperiale, University of Michigan-Ann Arbor

This is a work of the U.S. Government and is not subject to copyright protection in the United States. Foreign copyrights may apply.

Address correspondence to Tony T. Wang, Tony.Wang@fda.hhs.gov.

Received 3 June 2021

Accepted 4 June 2021

Published 16 June 2021

TABLE 1 Infection history of hamsters and neutralizing antibody titers at the time of rechallenge^a

Hamster ID	Date (mo/day/yr)			NAb titer (prechallenge)
	DOB	DOI-1	DOI-2	
WH033	7/12/2019	5/27/2020	2/1/2021	160
WH034	7/12/2019	5/27/2020	2/1/2021	80
WH095	4/17/2020	8/10/2020	2/1/2021	160
WH096	4/17/2020	8/10/2020	2/1/2021	80
WH097	4/17/2020	8/10/2020	2/1/2021	80
WH098	4/17/2020	8/10/2020	2/1/2021	160
WH080	9/1/2019	12/28/2020	2/1/2021	320
WH103	4/17/2020	12/28/2020	2/1/2021	320
WH194	12/1/2019	12/28/2020	2/1/2021	160
WH091	9/1/2019	12/28/2020	2/1/2021	80
WH079	9/1/2019	12/28/2020	2/1/2021	320
WH101	4/17/2020	12/28/2020	2/1/2021	160

^aAbbreviations: ID, identifier; DOB, date of birth; DOI-1, date of first infection; DOI-2, date of second infection; NAb, neutralizing antibody.

been found to increase the binding affinity of spike protein to the human ACE2 receptor, resulting in an elevated transmissibility and monoclonal antibody resistance (8–10).

Here, we set out to address whether a prior exposure to an ancestral SARS-CoV-2 (D614) isolate would offer protection against reinfection by a B.1.1.7 variant. In addition, we investigated whether the B.1.1.7 variant displays fitness advantage over the G614 variant in the Syrian hamster model.

One group of convalescent (previously infected with isolate USA-WA1/2020) and one group of naive hamsters ($n = 12$ per group, age paired) were intranasally inoculated with 10^4 PFU of a U.S. B.1.1.7 variant (isolate CA_CDC_5574/2020, termed CA B.1.1.7). A third group of 12 naive hamsters ($n = 12$) were similarly infected with a B.1 variant (isolate New York-PV08410/2020, termed NY B.1). The circulating neutralizing antibody titers in the 12 convalescent hamsters ranged from 80 to 320 at the time of challenge (Table 1), determined by a pseudovirus neutralization assay as previously described (11, 12). Nasal wash (NW) samples taken from infected hamsters on days 1, 2, and 3 postinfection (p.i.) showed that all hamsters contained detectable subgenomic RNA (sgRNA) levels in the nasal cavities on the first 2 days p.i. (Fig. 1A). Three days following infection, viral sgRNA levels from nasal washes of convalescent hamsters declined to below the detection limit, indicating that convalescent hamsters quickly controlled B.1.1.7 replication just as they controlled the reinfection with homologous viruses (11, 13, 14). In contrast, naive hamsters that were challenged with either the B.1.1.7 or B.1 variant showed 2- to 3- \log_{10} -higher levels of sgRNA than the convalescent group. Furthermore, naive hamsters that were challenged with the B.1.1.7 variant displayed overall higher levels of sgRNA in NW samples (statistically significant at day 2 p.i.) than those of the NY B.1-infected group. The same NW samples were also quantified for infectivity by a 50% tissue culture infectious dose (TCID₅₀) endpoint dilution assay (Fig. 1B). Only 3 out of 12 NW samples from convalescent hamsters exhibited detectable levels of infectious virus at day 1 p.i., dropping to below detection at day 2 p.i. (Fig. 1B). Surprisingly, NW samples from NY B.1-infected hamsters contained significantly higher TCID₅₀ values than those from CA B.1.1.7-infected hamsters on days 2 and 3 p.i. (Fig. 1B). To track the viral loads in the lung, we performed RNAscope on fixed lung tissues collected at 2 days postinfection (dpi), 4 dpi, and 7 dpi using a probe recognizing both NY B.1 and CDC B.1.1.7 variants (see Fig. S1 in the supplemental material). After quantification using Image J software, it was noted that NY B.1 viral RNA levels were higher than the CDC B.1.1.7 variant in the lung, at least at 2 and 7 dpi (Fig. S2). This observation suggests that the B.1.1.7 variant does not display fitness advantage over the B.1 variant in hamster lungs.

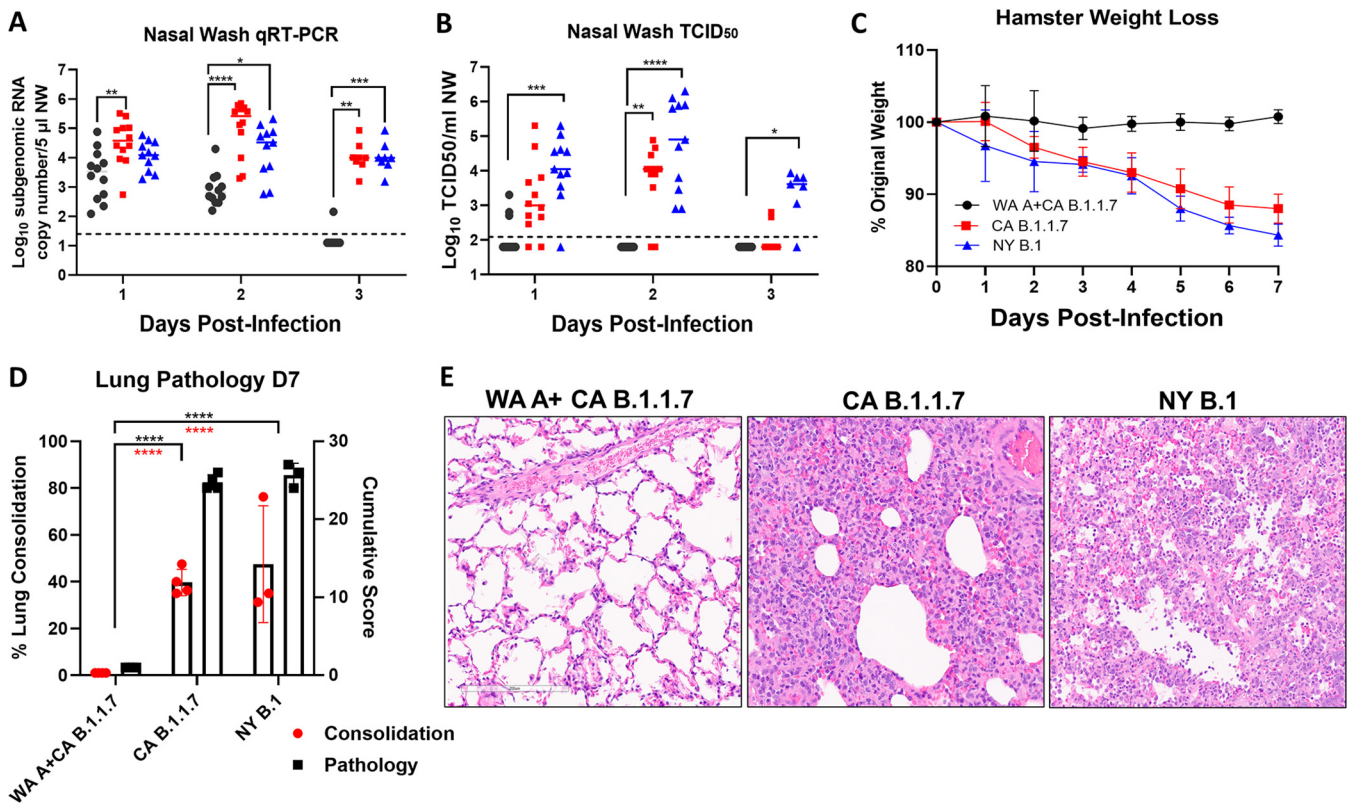


FIG 1 Convalescent hamsters are protected against severe disease from B.1.1.7 challenge. (A) Viral sgRNA titers in nasal wash samples taken from hamsters on days 1 to 3 postinfection. (B) Shedding of infectious virus in nasal wash samples determined by a TCID₅₀ assay. (C) Average weight loss was calculated based on initial weight taken on day 0 (day of infection). For panels A to C, symbols are defined in panel C. (D) Average pathology and consolidation scores for lung samples harvested at 7 dpi. (E) Representative images of hematoxylin and eosin staining of WA A+ CA B.1.1.7 (convalescent group) and CA B.1.1.7- and NY B.1-infected animals. Data points represent values from single samples; bars represent means and standard deviations (STD). Statistical significance is depicted as follows: *, *P* < 0.05; **, *P* < 0.01; ***, *P* < 0.001; ****, *P* < 0.0001.

Convalescent hamsters experienced no weight loss compared to the naive infected groups over the course of 7 dpi (Fig. 1C). Both the CA B.1.1.7- and NY B.1-infected animals lost 10 to 15% of body weight by day 7 p.i. At day 7 p.i., infected hamster lungs displayed pathology including alveolar wall thickening, airway infiltrates, perivascular edema, and hyperplasia (Fig. 1D and E). However, convalescent hamsters that were subsequently reinfected did not show these signature pathologies in the lungs (Fig. 1E). The cumulative pathology score and percentage of lung consolidation in the CA B.1.1.7 and NY B.1 naive groups had no significant difference (Fig. 1D), but both had significantly higher scores than those of convalescent hamsters (Fig. 1D). Therefore, although B.1.1.7 SARS-CoV-2 variant replication was higher in the nasal cavity on days 1 and 2 p.i. compared to the NY B.1 variant measured by sgRNA, the associated pathology was not more severe in the lung.

To account for the discrepancy between sgRNA titers and TCID₅₀ titers in NW samples, a second study using 10 male Syrian hamsters was subsequently performed. This study included two convalescent hamsters that were subsequently infected by CA B.1.1.7 and four naive NY B.1- and four naive CA B.1.1.7-infected Syrian hamsters aged >10 months. Again, NW samples of the CA B.1.1.7-infected hamsters show overall higher levels of sgRNA but slightly lower levels of infectious virus than those of NY B.1-infected animals (Fig. 2A and B). Tissue samples taken from convalescent hamsters at 4 dpi revealed 3- to 4-log₁₀-lower levels of sgRNA in all five lobes of the lung, trachea, and nasal turbinate (NT) in comparison to those from naive hamsters challenged with either the CA B.1.1.7 variant or the NY B.1 variant (Fig. 2C). Again, the degree of reduction in viral loads is comparable to what was observed in homologously rechallenged convalescent hamsters (11). Lung and NT homogenates were also titrated by plaque-forming assay in Vero E6 cells (Fig. 2D). Homogenates taken from convalescent hamsters contained no detectable infectious virus

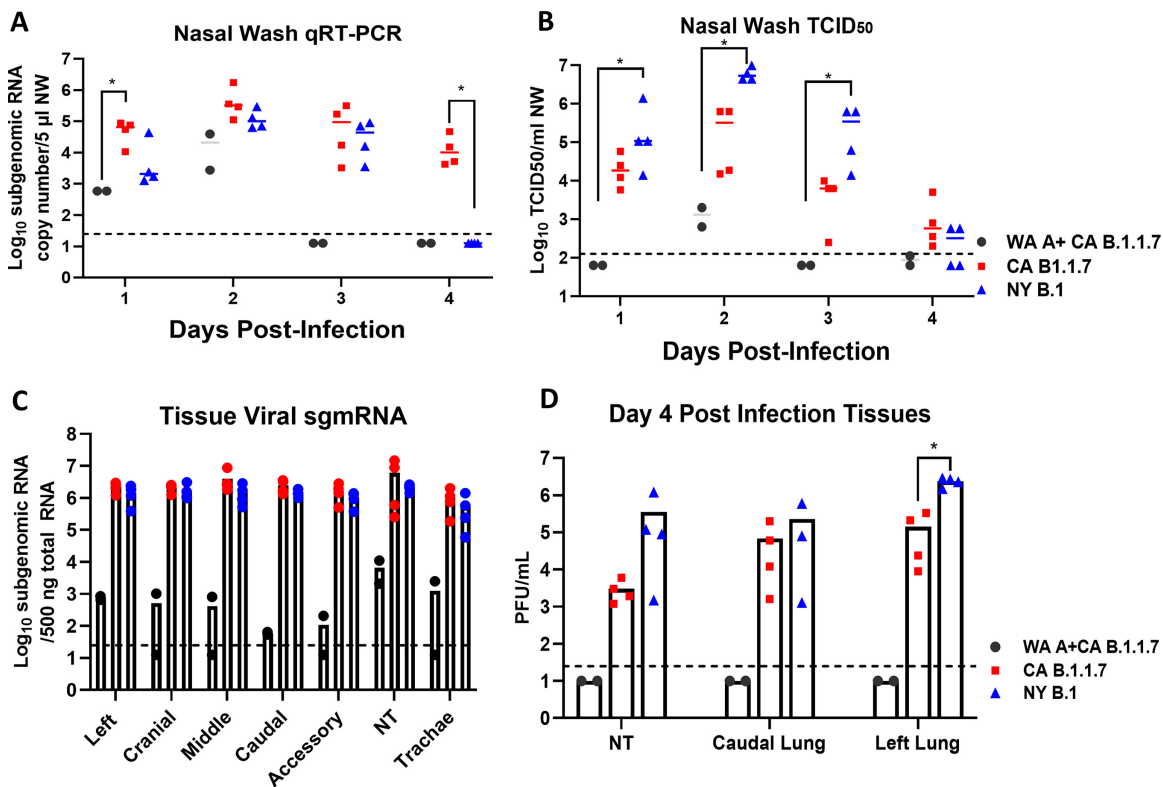


FIG 2 The SARS-CoV-2 B.1.1.7 variant is not more pathogenic than the ancestral G614 variant. (A) Viral sgRNA titers in nasal wash samples taken from hamsters from days 1 to 4 p.i. (B) TCID₅₀ values of the same samples as in panel A. (C) Five lobes of lung (left, cranial, middle, caudal, and accessory), NT, and trachea tissues were collected 4 days postinfection in 10 hamsters, and sgRNA (E gene) was measured via qRT-PCR. (D) Infectious titers of NT and lung homogenates (4 dpi) measured by plaque assay. Dots represent single samples; bars represent means and standard deviations. Statistical significance is depicted as follows: *, $P < 0.05$; **, $P < 0.01$; ***, $P < 0.001$; ****, $P < 0.0001$.

at 4 dpi. Interestingly, NY B.1-infected hamsters showed significantly higher infectious viral titers than CA B.1.1.7-challenged hamsters (Fig. 2D).

We and others have previously demonstrated that prior SARS-CoV-2 infections induced protective immunity in Syrian hamsters against a homologous rechallenge (11, 13, 14). This study finds that convalescent hamsters are protected against interstitial pneumonia following B.1.1.7 variant rechallenge and that the SARS-CoV-2 B.1.1.7 variant does not appear to be more pathogenic in adult male Syrian hamsters than the B.1 variant (D614G). Notably, breakthrough infections have now been observed in the nose on day 1 or 2 postchallenge with either a homologous (11) or a heterologous SARS-CoV-2 isolate (this study) in a small percentage of the convalescent hamsters despite the lung being completely protected from active viral replication. Difference in viral fitness may exist between the B.1.1.7 and B.1 variants in human beings; however, it was not conclusively observed in Syrian hamsters under the current experimental setting. On one hand, nasal wash samples from hamsters infected by a B.1.1.7 variant exhibited slightly higher viral RNA titers, which suggests higher levels of virus replication in the nasal cavity. On the other hand, infectious titers from the same nasal wash samples or lung homogenates of B.1.1.7 variant-infected animals were noticeably lower than those from B.1 (G614) variant-infected hamsters, arguing that Syrian hamsters may not fully recapitulate the B.1.1.7 infection in humans. Such a discrepancy of viral replication and infectious particles may be attributed to a disadvantaged B.1.1.7 plaquing effect in Vero E6 cells which has been previously mentioned (15), which would lead to undercounting of the B.1.1.7 variant in Vero E6 cells. To determine whether the B.1.1.7 variant undergoes deleterious changes in hamsters that would alter the overall infectivity of the virus, we also performed next-generation sequencing

TABLE 2 Summary of mutations found in variants propagated in-house or from hamster nasal washes (P1)^a

Mutation found in variant:				
BEI hCoV-19/USA/CA_CDC_5574/2020	In-house strain hCoV-19/USA/CA_CDC_5574/2020	Hamster P1 hCoV-19/USA/CA_CDC_5574/2020	In-house New York-PV08410/2020	Hamster P1 New York-PV08410/2020
Spike A570D	Spike A570D	Spike A570D		
Spike D614G	Spike D614G	Spike D614G	Nsp2 T85I	Nsp2 T85I (6/8)
Spike D1118H	Spike D1118H	Spike D1118H	Nsp12 P323L	Nsp12 P323L
Spike H69del	Spike H69del	Spike H69del	Spike D614G	Spike D614G
Spike N501Y	Spike N501Y	Spike N501Y	ORF3aQ57H	ORF3aQ57H (6/8)
Spike P681H	Spike P681H	Spike P681H	ORF8 S84L	ORF8 S84L (0/8)
Spike S982A	Spike S982A	Spike S982A		
Spike T716I	Spike T716I	Spike T716I (6/8)		
Spike V70del	Spike V70del	Spike V70del		
Spike Y145del	Spike Y145del	Spike Y145del		
M V70L	M V70L	M V70L (2/8)		
N D3L	N D3L	N D3L		
N G204R	N G204R	N G204R		
N R203K	N R203K	N R203K		
N S235F	N S235F	N S235F		
NS3 T223I	NS3 T223I	NS3 T223I		
NS8 Q27stop	NS8 Q27stop	NS8 Q27stop		
NS8 R52I	NS8 R52I	NS8 R52I		
NS8 Y73C	NS8 Y73C	NS8 Y73C		
NSP3 A890D	NSP3 A890D	NSP3 A890D		
NSP3 I1412T	NSP3 I1412T	NSP3 I1412T		
NSP3 T183I	NSP3 T183I	NSP3 T183I (7/8)		
NSP6 F108del	NSP6 F108del	NSP6 F108del		
NSP6 G107del	NSP6 G107del	NSP6 G107del		
NSP6 S106del	NSP6 S106del	NSP6 S106del		
NSP12 P323L	NSP12 P323L	NSP12 P323L		
NSP13 A454V	NSP13 A454V	NSP13 A454V		
NSP13 K460R	NSP13 K460R	NSP13 K460R		

^aThe numbers in parentheses (highlighted in bold) indicate the number of samples that contain the mutation. For example, **(6/8)** indicates that 6 out of 8 samples contained this mutation.

of 16 hamster NW samples (8 from B.1.1.7-infected and 8 from B.1-infected hamsters) (Table 2). All sequences retain >99.99% identity with the sequence of the input virus. Interestingly, both the sgRNA and infectious titers of NW samples from the B.1.1.7-infected hamsters are higher than those of the NY B.1-infected hamsters at day 4 p.i. This finding may suggest a prolonged viral shedding of B.1.1.7, which has been hypothesized to increase the transmissibility of the B.1.1.7 strain in the human population (10, 16). However, this study did not find any increase in pathogenicity of the B.1.1.7 variant in hamsters. The significance of the increased replication of the B.1.1.7 variant in the nasal cavity warrants further exploration through transmission studies.

Virus and cell culture. SARS-CoV-2 isolate hCoV-19/USA/CA_CDC_5574/2020 (B.1.1.7) and SARS-CoV-2/human/USA/NY-PV08410/2020 (B.1) were propagated in Vero E6 cells to generate working virus stocks with infectious titers of 4.7×10^6 PFU/ml and 1.8×10^7 PFU/ml, respectively, and sequenced to confirm genotypes. SARS-CoV-2 isolate hCoV-19/USA/CA_CDC_5574/2020 differs from the original U.K. B.1.1.7 variant by three mutations (M/V70L, NS3/T223I), and NSP13/A454V).

SARS-CoV-2 pseudovirus production and neutralization assay. Human codon-optimized cDNA encoding SARS-CoV-2 S glycoprotein (NC_045512) was synthesized by GenScript and cloned into eukaryotic cell expression vector pcDNA 3.1 between the BamHI and XhoI sites. Pseudovirions were produced by cotransfection of Lenti-X 293T cells with psPAX2, pTRIP-luc, and SARS-CoV-2 S-expressing plasmid using Lipofectamine 3000. The supernatants were harvested at 48 and 72 h posttransfection and filtered through 0.45- μ m membranes. For the serum neutralization assay, 50 μ l of SARS-CoV-2 S pseudovirions was preincubated with an equal volume of medium containing serum at various dilutions at room temperature for 1 h, and then virus-antibody mixtures were added to 293T-hACE2 cells in a 96-well plate. After 3 h of incubation, the inoculum was

replaced with fresh medium. Cells were lysed 48 h later, and luciferase activity was measured using luciferin-containing substrate. Controls included cell-only control, a control consisting of virus without any antibody, and positive-control sera. The endpoint titers were calculated as the last serum dilution resulting in at least 50% SARS-CoV-2 neutralization. The amount of pseudovirions used in this assay has been determined to give rise to a target input of 5×10^5 to 5×10^7 relative light units (RLU)/ml, under which condition the neutralization law is observed.

Hamster challenge experiments. Procedures for hamster challenge experiments were as described previously (11, 12). For challenge studies, aged (10 to 12 months old) Syrian hamsters were anesthetized with 3 to 5% isoflurane. Intranasal inoculation was done with 10^4 PFU/hamster of SARS-CoV-2 in a 50- μ l volume dropwise into the nostrils. Nasal washes were collected by pipetting ~ 200 μ l sterile phosphate-buffered saline into one nostril. Male hamsters ($n = 12$) were divided into three groups. The first group contained hamsters who were previously infected with the USA-WA1/2020 variant (lineage A, GISAID clade S), which was circulating in Washington State in early 2020. The second group of hamsters were immunologically naive and were intranasally infected with the B.1.1.7 variant hCoV-19/USA/CA_CDC_5574/2020 (GISAID clade GR). The third group of hamsters were challenged with New York-PV08410/2020 (G614, B.1 lineage, GISAID clade GH). Following infection, hamsters were monitored for clinical signs and weight loss. Nasal wash samples taken on days 1, 2, and 3 postinfection (p.i.) to test for sgRNA and TCID₅₀. Seven days following infection, a subset of hamsters was humanely euthanized and lungs were taken for histopathology.

RNA isolation and qRT-PCR. Procedures for RNA isolation and reverse transcription-quantitative PCR (qRT-PCR) were as described previously (11, 12).

Next-generation sequencing. Detailed procedures have been published previously (12). To prepare sequencing libraries, 20 μ l RNA was extracted from 140 μ l virus stock or hamster lung homogenates. RNA quality was assessed by Agilent 2100 Bioanalyzer (Agilent Technologies, Santa Clara, CA, USA), and the RNA integrity numbers (RIN) were all greater than 9. A total of 8.5 μ l of the samples was used to prepare the sequencing library (2 μ l was used to check the RNA quality and size, and 6.5 μ l was used for the library construction). Library preparation followed "Illumina section 2 c) Illumina shotgun metagenomics" (https://github.com/CDCgov/SARS-CoV-2_Sequencing). If the RNA was derived from virus stocks, approximately <19% of total reads were mapped to African green monkey cells (the host cell) even without depletion of rRNA. Therefore, omission of the rRNA removal still yielded enough reads mapped to SARS-CoV-2 (~ 50 to 75% of total reads). In the Illumina protocol, rRNA removal was usually included if the RNA was derived from tissues but was omitted in this study without affecting the quality of the sequence because we have found that the use of the enrichment-based Illumina sample prep kit yielded similar results as when the rRNA removal step (metagenomic approach) was included. The Illumina sample prep kit (enrichment-based) captures several human respiratory viruses (including SARS-CoV-2). Prepared libraries were loaded onto the NextSeq sequencer for deep sequencing. The reference sequence is coronavirus 2 isolate Wuhan-Hu-1 (GenBank accession no. [MN908947.3](https://www.ncbi.nlm.nih.gov/nuccore/MN908947.3)). Variant calling is done by the CLC Genomics Workbench V20 low-frequency variant detection (Qiagen) with the requirement of significance of $\geq 5\%$ and minimum frequency of $\geq 20\%$. We got roughly 500,000 to 900,000 reads per virus sample, each read containing 75 bp. If using the SARS-CoV-2 genome ($\sim 30,000$ bp) to estimate, the coverage was about $1,250\times$ to $2,250\times$, assuming the reads were distributed equally. In practice, we noticed the C-terminal region has more reads than other regions.

Histopathology and RNAscope analyses. Procedures for histology and RNAscope analyses were as described previously (11, 12). See Table S1 in the supplemental material for the pathology scoring sheet.

TCID₅₀. Procedures for the TCID₅₀ assay were as described previously (11, 12).

Plaque assay. Nasal wash samples were 10-fold serially diluted and added to a 6-well plate with Vero E6 cells. After 1 h, the mixture was removed and replenished with tragacanth gum overlay (final concentration 0.3%). Cells were incubated at 37°C and

5% CO₂ for 2 days and then fixed with 4% paraformaldehyde, followed by staining of cells with 0.1% crystal violet in 20% methanol for 5 to 10 min.

Statistical analysis. All statistical analysis was performed using one-way analysis of variance (ANOVA) (Kruskal-Wallis) nonparametric tests, followed by a *post hoc* Tukey analysis on GraphPad Prism (8.4.2) software for Windows (GraphPad Software, San Diego, CA, USA). Statistical significance is depicted as follows: *, $P < 0.05$; **, $P < 0.01$; ***, $P < 0.001$; ****, $P < 0.0001$.

SUPPLEMENTAL MATERIAL

Supplemental material is available online only.

FIG S1, TIF file, 1.7 MB.

FIG S2, JPG file, 1.7 MB.

TABLE S1, DOCX file, 0.02 MB.

ACKNOWLEDGMENTS

We thank the White Oak FDA Animal Program staff and veterinarians: John Dennis, Mario Hernandez, Mario Ortega, and Eric Nimako. We thank Katherine Shea for assistance with scanning pathology slides. We are grateful to W. Wu and C.-K. Chou for help with next-generation sequencing of viral RNA. The following reagents were deposited by the Centers for Disease Control and Prevention and obtained through Biodefense and Emerging Infections Research Resources Repository, NIAID, NIH: SARS-related coronavirus 2, isolate USA-WA1/2020, NR-52281; isolate USA/CA_CDC_5574/2020, NR-54011; isolate New York-PV08410/2020, NR-53514.

The work described in this paper was supported by US FDA intramural grant funds. The funders had no role in study design, data collection and analysis, decision to publish, or preparation of the manuscript.

The content of this publication does not necessarily reflect the views or policies of the Department of Health and Human Services, nor does mention of trade names, commercial products, or organizations imply endorsement by the US Government.

Author contributions: Ivette A. Nuñez, formal analysis, investigation, writing—original draft, visualization; Christopher Z. Lien, investigation; Prabhuanand Selvaraj, methodology, investigation; Charles B. Stauff, investigation; Shufeng Liu, methodology, investigation; Matthew F. Starost, investigation; Tony T. Wang, conceptualization, methodology, investigation, writing—original draft, visualization, supervision, project administration.

There are no competing interests.

REFERENCES

- Sevajol M, Sibissi L, Decroly E, Canard B, Imbert I. 2014. Insights into RNA synthesis, capping, and proofreading mechanisms of SARS-coronavirus. *Virus Res* 194:90–99. <https://doi.org/10.1016/j.virusres.2014.10.008>.
- Piccoli L, Park Y-J, Tortorici MA, Czudnochowski N, Walls AC, Beltramello M, Silacci-Fregni C, Pinto D, Rosen LE, Bowen JE, Acton OJ, Jaconi S, Guarino B, Minola A, Zatta F, Sprugasci N, Bassi J, Peter A, De Marco A, Nix JC, Mele F, Jovic S, Rodriguez BF, Gupta SV, Jin F, Piumatti G, Lo Presti G, Pellanda AF, Biggiogero M, Tarkowski M, Pizzuto MS, Cameroni E, Havenar-Daughton C, Smithey M, Hong D, Lepori V, Albanese E, Ceschi A, Bernasconi E, Elzi L, Ferrari P, Garzoni C, Riva A, Snell G, Sallusto F, Fink K, Virgin HW, Lanzavecchia A, Corti D, Velesler D. 2020. Mapping neutralizing and immunodominant sites on the SARS-CoV-2 spike receptor-binding domain by structure-guided high-resolution serology. *Cell* 183:1024–1042.e21. <https://doi.org/10.1016/j.cell.2020.09.037>.
- Walls AC, Park Y-J, Tortorici MA, Wall A, McGuire AT, Velesler D. 2020. Structure, function, and antigenicity of the SARS-CoV-2 spike glycoprotein. *Cell* 181:281–292.e6. <https://doi.org/10.1016/j.cell.2020.02.058>.
- Wrapp D, Wang N, Corbett KS, Goldsmith JA, Hsieh C-L, Abiona O, Graham BS, McLellan JS. 2020. Cryo-EM structure of the 2019-nCoV spike in the prefusion conformation. *Science* 367:1260–1263. <https://doi.org/10.1126/science.abb2507>.
- Tortorici MA, Velesler D. 2019. Structural insights into coronavirus entry. *Adv Virus Res* 105:93–116. <https://doi.org/10.1016/bs.aivir.2019.08.002>.
- Isabel S, Graña-Miraglia L, Gutierrez JM, Bundalovic-Torma C, Groves HE, Isabel MR, Eshaghi A, Patel SN, Gubbay JB, Poutanen T, Guttman DS, Poutanen SM. 2020. Evolutionary and structural analyses of SARS-CoV-2 D614G spike protein mutation now documented worldwide. *Sci Rep* 10:14031. <https://doi.org/10.1038/s41598-020-70827-z>.
- Rambaut A, Loman N, Pybus O, Barclay W, Barrett J, Carabelli A, Connor T, Peacock T, Robertson D, Volz E. 2020. Preliminary genomic characterisation of an emergent SARS-CoV-2 lineage in the UK defined by a novel set of spike mutations. <https://virological.org/t/preliminary-genomic-characterisation-of-an-emergent-sars-cov-2-lineage-in-the-uk-defined-by-a-novel-set-of-spike-mutations/563>.
- Wang P, Nair MS, Liu L, Iketani S, Luo Y, Guo Y, Wang M, Yu J, Zhang B, Kwong PD, Graham BS, Mascola JR, Chang JY, Yin MT, Sobieszczak M, Kyratsous CA, Shapiro L, Sheng Z, Huang Y, Ho DD. 2021. Antibody resistance of SARS-CoV-2 variants B.1.351 and B.1.1.7. *bioRxiv* <https://doi.org/10.1101/2021.01.25.428137>.
- Volz E, Mishra S, Chand M, Barrett JC, Johnson R, Geidelberg L, Hinsley WR, Laydon DJ, Dabrera G, O'Toole Á, Amato R, Ragonnet-Cronin M, Harrison I, Jackson B, Ariani CV, Boyd O, Loman NJ, McCrone JT, Gonçalves S, Jorgensen D, Myers R, Hill V, Jackson DK, Gaythorpe K, Groves N, Sillitoe J, Kwiatkowski DP, Flaxman S, Ratmann O, Bhatt S, Hopkins S, Gandy A, Rambaut A, Ferguson NM. 2021. Transmission of SARS-CoV-2 lineage B.1.1.7 in England: insights from linking epidemiological and genetic data. *medRxiv* <https://doi.org/10.1101/2020.12.30.20249034>.

10. Davies NG, Abbott S, Barnard RC, Jarvis CI, Kucharski AJ, Munday JD, Pearson CAB, Russell TW, Tully DC, Washburne AD, Wenseleers T, Gimma A, Waites W, Wong KLM, van Zandvoort K, Silverman JD, Diaz-Ordaz K, Keogh R, Eggo RM, Funk S, Jit M, Atkins KE, Edmunds WJ, CMMID COVID-19 Working Group. 2021. Estimated transmissibility and impact of SARS-CoV-2 lineage B.1.1.7 in England. *Science* 372:eabg3055. <https://doi.org/10.1126/science.abg3055>.
11. Selvaraj P, Lien CZ, Liu S, Stauf CB, Nunez IA, Hernandez M, Nimako E, Ortega MA, Starost MF, Dennis JU, Wang TT. 2021. SARS-CoV-2 infection induces protective immunity and limits transmission in Syrian hamsters. *Life Sci Alliance* 4:e202000886. <https://doi.org/10.26508/lsa.202000886>.
12. Stauf CB, Lien CZ, Selvaraj P, Liu S, Wang TT. 2021. The G614 pandemic SARS-CoV-2 variant is not more pathogenic than the original D614 form in adult Syrian hamsters. *Virology* 556:96–100. <https://doi.org/10.1016/j.virol.2021.01.005>.
13. Brustolin M, Rodon J, Rodriguez de la Concepcion ML, Avila-Nieto C, Cantero G, Perez M, Te N, Noguera-Julian M, Guallar V, Valencia A, Roca N, Izquierdo-Useros N, Blanco J, Clotet B, Bensaid A, Carrillo J, Vergara-Alert J, Segales J. 2021. Protection against reinfection with D614- or G614-SARS-CoV-2 isolates in golden Syrian hamster. *Emerg Microbes Infect* 10:797–809. <https://doi.org/10.1080/22221751.2021.1913974>.
14. Imai M, Iwatsuki-Horimoto K, Hatta M, Loeber S, Halfmann PJ, Nakajima N, Watanabe T, Ujie M, Takahashi K, Ito M, Yamada S, Fan S, Chiba S, Kuroda M, Guan L, Takada K, Armbrust T, Balogh A, Furusawa Y, Okuda M, Ueki H, Yasuhara A, Sakai-Tagawa Y, Lopes TJS, Kiso M, Yamayoshi S, Kinoshita N, Ohmagari N, Hattori SI, Takeda M, Mitsuya H, Krammer F, Suzuki T, Kawaoka Y. 2020. Syrian hamsters as a small animal model for SARS-CoV-2 infection and countermeasure development. *Proc Natl Acad Sci U S A* 117:16587–16595. <https://doi.org/10.1073/pnas.2009799117>.
15. Brown JC, Goldhill DH, Zhou J, Peacock TP, Frise R, Goonawardane N, Baillon L, Kugathasan R, Pinto AL, McKay PF, Hassard J, Moshe M, Singanayagam A, Burgoyne T, Barclay WS. 2021. Increased transmission of SARS-CoV-2 lineage B.1.1.7 (VOC 202012/01) is not accounted for by a replicative advantage in primary airway cells or antibody escape. *bioRxiv* <https://doi.org/10.1101/2021.02.24.432576>.
16. Kissler SM, Fauver JR, Mack C, Tai C, Breban M, Watkins AE, Samant R, Anderson D, Ho D, Grubaugh ND, Grad YH. 2021. Densely sampled viral trajectories suggest longer duration of acute infection with B.1.1.7 variant relative to non-B.1.1.7 SARS-CoV-2. *medRxiv*. <https://doi.org/10.1101/2021.02.16.21251535>.